Tokyo Climate Center, Japan Meteorological Agency

TCC News

No. 46 Autumn 2016

Contents	Page

El Niño Outlook (November 2016 - May 2017)

The likelihood of La Niña conditions persisting throughout boreal winter (60%) is higher than that of ENSO-neutral conditions returning (40%). (Article based on El Niño outlook issued on 10 November 2016.)

El Niño/La Niña

In October 2016, the NINO.3 SST was below normal with a deviation of -0.5°C. SSTs (Figures 1 and 3 (a)) were below normal in the central and eastern equatorial Pacific, and above normal in the western part. Subsurface temperatures were below normal in the central and eastern equatorial Pacific (Figures 2 and 3 (b)). Atmospheric convective activity was below normal near the date line over the equatorial Pacific, and easterly winds in the lower troposphere (trade winds) were stronger than normal over the central part. These oceanic and atmospheric conditions are consistent with common patterns seen in the past La Niña events. As they are expected to continue in the coming months, La Niña conditions can be considered present in the equatorial Pacific.

The persistent subsurface cold waters observed in the central equatorial Pacific from July onward were stronger in October than in September. These waters are expected to produce ongoing cooler-than-normal sea surface conditions in the central equatorial Pacific during the months ahead. JMA's El Niño prediction model suggests that the NINO.3 SST will be below normal in boreal autumn and near or below normal in boreal winter (Figure 4). In conclusion, the likelihood of La Niña conditions persisting throughout boreal winter (60%) is higher than that of ENSO-neutral conditions returning (40%) (Figure 5).

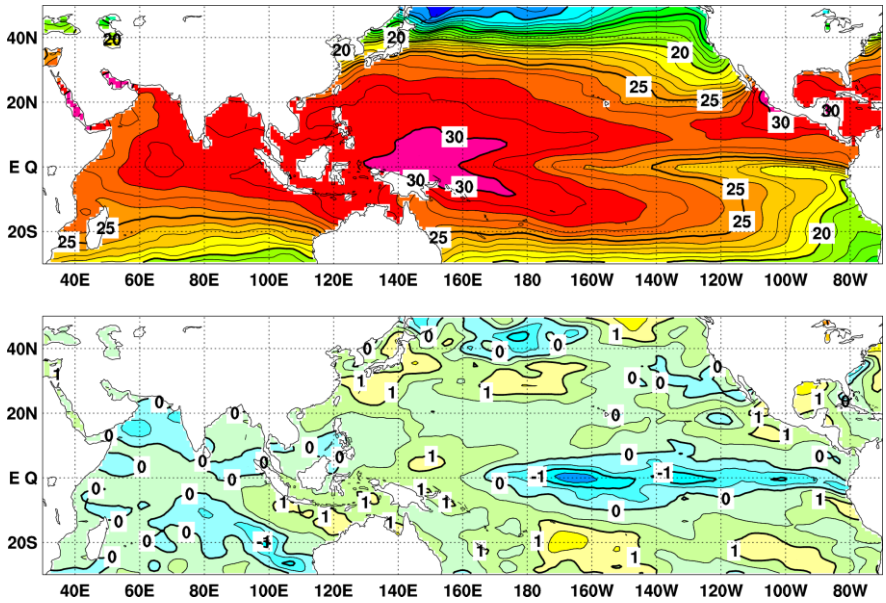

Figure 1
Monthly mean (a) sea surface temperatures (SSTs) and (b) SST anomalies in the Indian and Pacific Ocean areas for October 2016
The contour intervals are 1˚C in (a) and 0.5˚C in (b). The base period for the normal is 1981 – 2010.

Western Pacific and Indian Ocean

The area-averaged SST in the tropical western Pacific (NINO.WEST) region was above normal in October, and is likely to be above normal until boreal winter.

The area-averaged SST in the tropical Indian Ocean (IOBW) region was below normal in October, and is likely to be below normal in boreal autumn and near or below normal in boreal winter.

Impacts

The ongoing La Niña conditions are considered to have caused the warmer-than-normal conditions observed in Western Japan and Okinawa/Amami and as well as the shorter-than-normal sunshine durations observed in Western Japan in October 2016.

In the same month, warmer-than-normal conditions in the eastern part of the Unites States were consistent with common patterns observed in past La Niña events.

(Ichiro Ishikawa, Climate Prediction Division)

* The SST normal for the NINO.3 region (5°S – 5°N, 150°W – 90°W) is defined as an monthly average over the latest sliding 30-year period (1986-2015 for this year).

* The SST normals for the NINO.WEST region (Eq. – 15°N, 130°E – 150°E) and the IOBW region (20°S – 20°N, 40°E – 100°E) are defined as linear extrapolations with respect to the latest sliding 30-year period, in order to remove the effects of significant long-term warming trends observed in these regions.

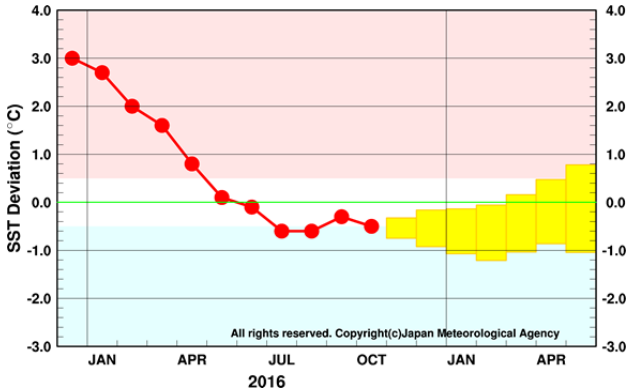

Figure 4 Outlook of NINO.3 SST deviation produced by the El Niño prediction model

This figure shows a time series of monthly NINO.3 SST deviations. The thick line with closed circles shows observed SST deviations, and the boxes show the values produced for up to six months ahead by the El Niño prediction model. Each box denotes the range into which the SST deviation is expected to fall with a probability of 70%.

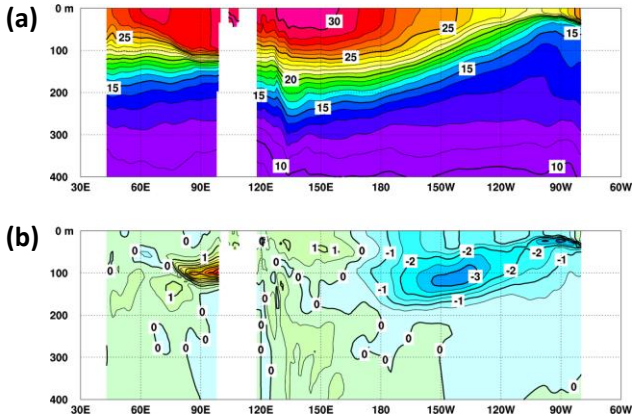

Figure 2 Monthly mean depth-longitude cross sections of (a) temperatures and (b) temperature anomalies in the equatorial Indian and Pacific Ocean areas for October 2016

The contour intervals are 1˚C in (a) and 0.5˚C in (b). The base period for the normal is 1981 – 2010.

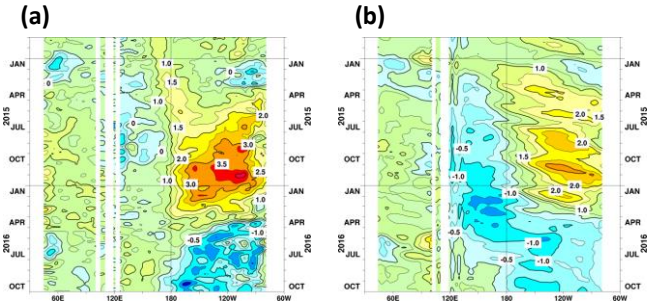

Figure 3 Time-longitude cross sections of (a) SST and (b) ocean heat content (OHC) anomalies along the equator in the Indian and Pacific Ocean areas

OHCs are defined here as vertical averaged temperatures in the top 300 m. The base period for the normal is 1981 – 2010.

YEAR	MONTH	mean period	El Niño	ENSO neutral	La Niña
2016	SEP	JUL2016–NOV2016	10		90
	OCT	AUG2016–DEC2016	30		70
	NOV	**SEP2016–JAN2017**	30		70
	DEC	**OCT2016–FEB2017**	40		60
2017	**JAN**	**NOV2016–MAR2017**	40		60
	FEB	**DEC2016–APR2017**	50		50
	MAR	**JAN2017–MAY2017**	60		40

Figure 5 ENSO forecast probabilities based on the El Niño prediction model

Red, yellow and blue bars indicate probabilities that the five-month running mean of the NINO.3 SST deviation from the latest sliding 30-year mean will be +0.5°C or above (El Niño), between +0.4 and -0.4°C (ENSO-neutral) and -0.5°C or below (La Niña), respectively. Regular text indicates past months, and bold text indicates current and future months.

JMA's Seasonal Numerical Ensemble Prediction for Boreal Winter 2016/2017

Based on JMA's seasonal ensemble prediction system, sea surface temperature (SST) anomalies are predicted to be below normal in the equatorial Pacific Ocean this boreal winter, suggesting a likely persistence of La Niña conditions. In association with these oceanic conditions, inactive convection anomalies are predicted over the central Pacific. Conversely, active convection anomalies are predicted over the Maritime Continent. In association with these convection anomalies, equatorial symmetric cyclonic anomalies are predicted at the lower troposphere over the Maritime Continent, suggesting the likelihood of a stronger northeast winter monsoon than normal in Indochina.

1. Introduction

This article outlines JMA's dynamical seasonal ensemble prediction for boreal winter 2016/2017 (December - February, referred to as DJF), which was used as a basis for the Agency's operational cold-season outlook issued on 25 November 2016. The outlook detailed here is based on the seasonal ensemble prediction system of the Coupled atmosphere-ocean General Circulation Model (CGCM). See the column below for system details.

Section 2 outlines global SST anomaly predictions, and Section 3 describes the associated circulation fields expected over the tropics and sub-tropics. Finally, the circulation fields predicted for the mid- and high- latitudes of the Northern Hemisphere are discussed in Section 4.

2. SST anomalies (Figure 5)

Figure 5 shows predicted SSTs (contours) and related anomalies (shading) for DJF. SST anomalies are predicted to be below normal in the equatorial Pacific Ocean throughout the period, suggesting a likely persistence of La Niña conditions. Conversely, they are predicted to be above normal in most parts of the Maritime Continent. Additionally, they are predicted to be near normal in the Indian Ocean.

3. Prediction for the tropics and sub-tropics (Figure 6)

Figure 6 (a) shows predicted precipitations (contours) and related anomalies (shading) for DJF. In association with the

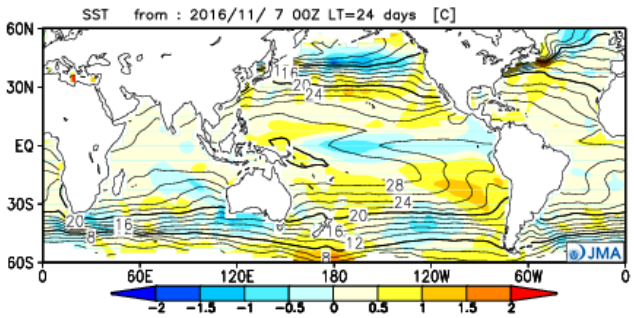

Figure 5 Predicted SSTs (contours) and SST anomalies (shading) for December–February 2016/2017 (ensemble mean of 51 members)

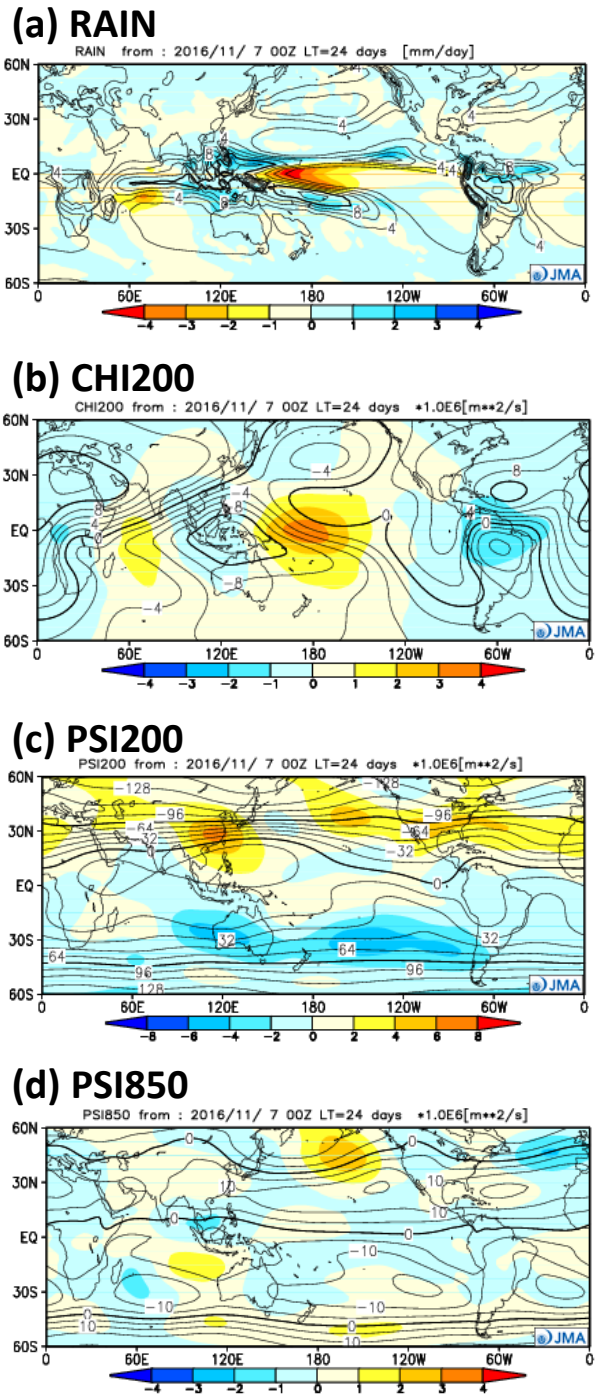

Figure 6 Predicted atmospheric fields from 60°N - 60°S for December-February 2016/2017 (ensemble mean of 51 members)

(a) Precipitation (contours) and anomaly (shading). The contour interval is 2 mm/day.

(b) Velocity potential at 200 hPa (contours) and anomaly (shading). The contour interval is 2×10^6 m^2/s.

(c) Stream function at 200 hPa (contours) and anomaly (shading). The contour interval is 16×10^6 m^2/s.

(d) Stream function at 850 hPa (contours) and anomaly (shading). The contour interval is 5×10^6 m^2/s.

oceanic conditions, precipitation anomalies are predicted to be below normal over the equatorial Pacific Ocean and above normal over the Maritime Continent.

Figure 6 (b) shows predicted velocity potentials (contours) and related anomalies (shading) for DJF in the upper troposphere (200hPa). Velocity potential anomalies at 200hPa are predicted to be positive (i.e., convergent) over the equatorial Pacific, reflecting inactive convection. Conversely, negative (i.e., divergent) anomalies are predicted over the Maritime Continent, reflecting active convection.

Figure 6 (c) shows predicted stream functions (contours) and related anomalies (shading) for DJF in the upper troposphere (200hPa). In association with the active convections over the Maritime Continent, stream function anomalies at 200hPa are predicted to be positive (i.e., anticyclonic) over Eurasia, indicating a northward-shifting tendency of the subtropical jet stream.

Figure 6 (d) shows predicted stream functions (contours) and related anomalies (shading) for DJF in the lower troposphere (850hPa). Equatorial Symmetric negative (i.e., cyclonic) anomalies at 850hPa are predicted over the Maritime Continent, suggesting the likelihood of a stronger northeast winter monsoon than normal in Indochina. Accordingly, normal or colder conditions are expected in Indochina despite resent global warming trends. These atmospheric characteristics are consistent with those observed in past La Niña events.

4. Prediction for the mid- and high- latitudes of the Northern Hemisphere (Figure 7)

Figure 7 (a) shows predicted geopotential heights (contours) and related anomalies (shading) for DJF at 500hPa. Geopotential height anomalies at 500hPa are predicted to be positive over most parts of Northern Hemisphere, reflecting resent global warming trends. Although strong positive anomalies are predicted over northern parts of South Asia and Southeast Asia and negative anomalies are predicted over the sea to the southeast of Japan, this information should be interpreted with caution due to inconsistency with the atmospheric characteristics observed in past La Niña events.

Figure 7 (b) shows predicted sea level pressures (contours) and related anomalies (shading) for DJF. Sea level pressure anomalies are predicted to be negative over most parts of Eurasia, suggesting a weaker Siberian High than normal. However, this should also be interpreted with caution due to inconsistency with the atmospheric characteristics observed in past La Niña events. Conversely, sea level pressure anomalies are predicted to be positive over the Bering Sea and offshore to the west of North America, suggesting a weaker than normal Aleutian Low in those regions. This is consistent with the atmospheric characteristics observed in past La Niña events.

(Takashi Yamada, Climate Prediction Division)

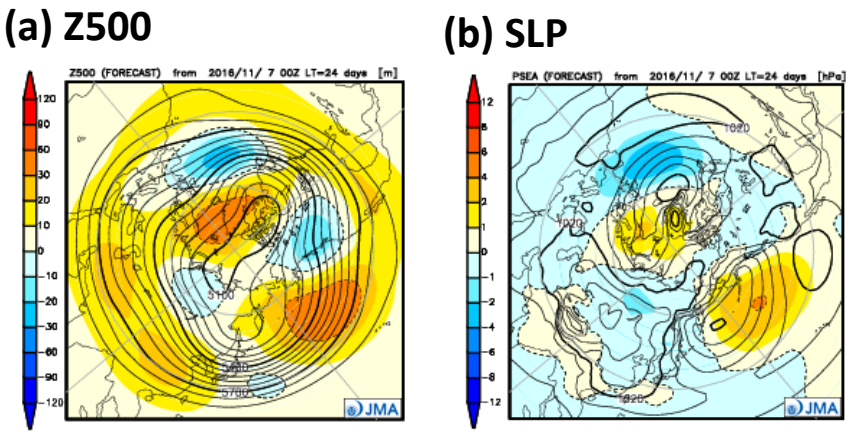

Figures 7 Predicted atmospheric fields from 20°N - 90°N for December–February 2016/2017 (ensemble mean of 51 members)

(a) Geopotential height at 500hPa (contours) and anomaly (shading). The contour interval is 60 m.
(b) Sea level pressure (contours) and anomaly (shading). The contour interval is 4hPa.

JMA's Seasonal Ensemble Prediction System

JMA operates a seasonal Ensemble Prediction System (EPS) using the Coupled atmosphere-ocean General Circulation Model (CGCM) to make seasonal predictions beyond a one-month time range. The EPS produces perturbed initial conditions by means of a combination of the initial perturbation method and the lagged average forecasting (LAF) method. The prediction is made using 51 members from the latest 4 initial dates (13 members are run every five days). Details of the prediction system and verification maps based on 30-year hindcast experiments (1981 - 2010) are available at http://ds.data.jma.go.jp/tcc/tcc/products/model/.

Cold Season Outlook for Winter 2016/2017 in Japan

JMA issued its outlook for the coming winter (December 2016 - February 2017) over Japan in September and updated it in October based on the Agency's seasonal Ensemble Prediction System (EPS). This article outlines the outlook update of 25 October.

1. Outlook summary (Figure 8)

In northern Japan, seasonal precipitation amounts and seasonal mean temperatures are expected to exhibit above-normal tendencies due to major influences relating to low-pressure systems and minor influences relating to cold-air advection from higher latitudes.

In western Japan and Okinawa/Amami, seasonal mean temperatures are expected to exhibit below-normal tendencies due to major influences relating to inflow of cold air from the continent. Seasonal snowfall amounts for the Sea of Japan side are expected to exhibit above-normal tendencies in western Japan.

2. Outlook background

Figure 9 highlights expected large-scale oceanic/atmospheric characteristics for winter. An outline of the background to the outlook is given below.

* Sea surface temperatures (SSTs) are expected to be below normal from the central to the eastern tropical Pacific and above normal in the western tropical Pacific. Accordingly, the likelihood of La Niña conditions persisting throughout boreal winter is higher than that of ENSO-neutral conditions returning.
* In association with the expected SST anomalies in the tropics, convection over the tropics is expected to be more active than normal around the Maritime Continent and less active than normal over the central Pacific.
* In upper circulation fields, anti-cyclonic anomalies are predicted over southern China in association with active convection over the Maritime Continent. Relatively cyclonic anomalies are predicted around northern Japan, which will be on the northeastern side of anticyclonic anomalies. Accordingly, upper-air westerlies are expected to meander northward around China and southward east of Japan.
* The Siberian High is expected to be stronger than normal in its southeastern part in association with anticyclonic anomalies over southern China, which would bring strong winter monsoon tendencies to southern Japan in particular.
* Around northern Japan, lower sea level pressure and stronger cyclonic anomalies are predicted, which would significantly influence low-pressure systems and create above-normal-precipitation tendencies. Meanwhile, the influences of cold northern air would tend to be minor in northern Japan with the weaker western (rather than northern) wind anomalies taken into account.
* Overall temperatures in the troposphere are expected to be higher than normal in association with the prevailing long-term trend. These tendencies are likely to increase the chance of above-normal temperatures.
* In consideration of the above, seasonal mean temperature tendencies are expected to be below normal in western Japan and Okinawa/Amami, near normal in eastern Japan and above normal in northern Japan.

(Masayuki Hirai, Climate Prediction Division)

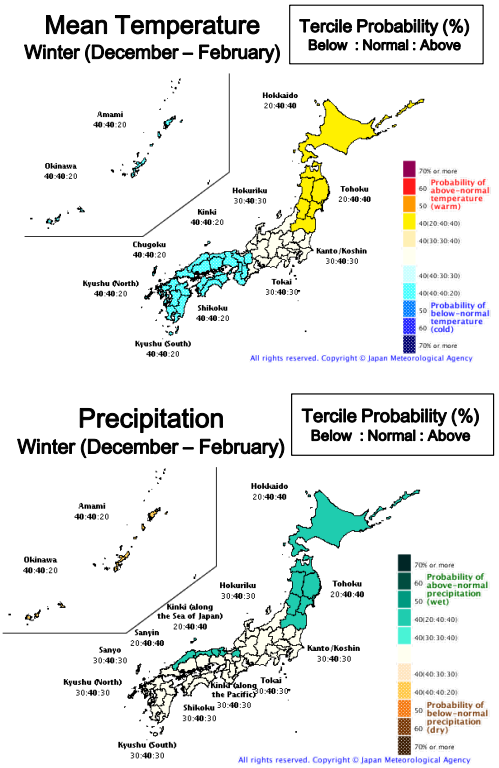

Figure 8 Outlook for winter 2016/2017 temperature (above) and precipitation (below) probability in Japan.

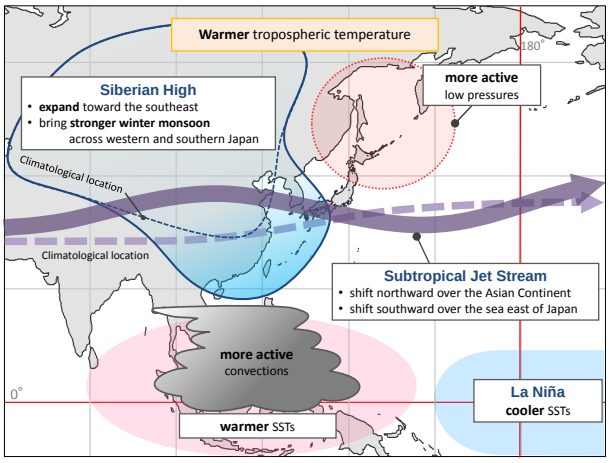

Figure 9 Schematic diagram showing expected large-scale ocean/atmosphere characteristics for winter 2016/2017

1. Precipitation and temperature

Four-month total precipitation amounts based on CLIMAT reports for the monsoon season (June – September) were more than 140% of the normal in the Hokkaido region of Japan, in eastern China, in southern Mongolia, in the area from northern Lao PDR to northern Myanmar, in and around northern Pakistan and in central Indonesia. Conversely, the corresponding figures were less than 60% of the normal on the Korean Peninsula, in northeastern and central China, in and around southern India and in southwestern Pakistan (Figure 10(a)). Remarkably high precipitation was seen over the mid- to downstream basin of the Yangtze River in China from June to August and in Hokkaido in August.

Four-month mean temperatures for the same period were more than 1°C above normal in many parts of East Asia especially north of 30°N, and were slightly below normal in parts of South Asia and Myanmar (Figure 10 (b)).

2. Tropical cyclones

The first named tropical cyclone (TC) of 2016 formed over the western North Pacific on July 3, making it the second-latest on record since 1951. Subsequently, however, the number of TC formations approached the normal. As of the end of September, there had been 18 TCs against a normal of 18.4. Six of these made landfall on Japan, which is the joint-second-highest number on record (after the 10 recorded in 2004).

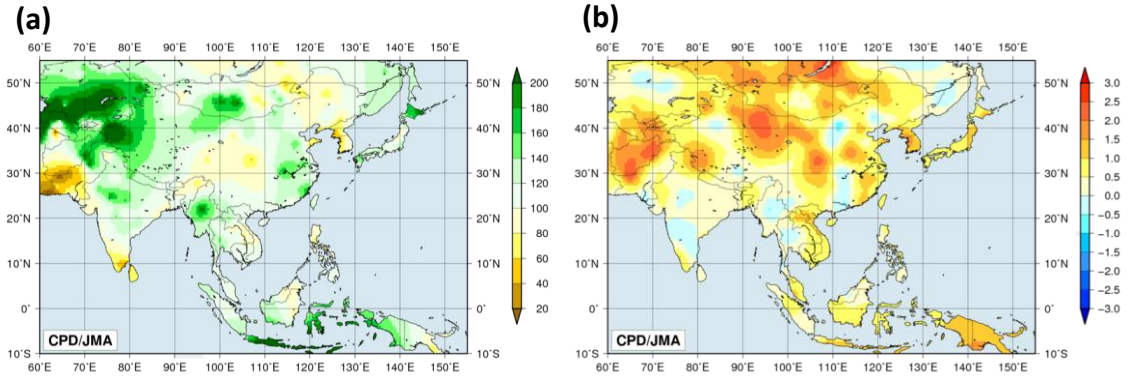

Figure 10 (a) Four-month precipitation ratios (%) from June to September 2016
(b) Four-month mean temperature anomalies (°C) from June to September 2016
The base period for normal is 1981 – 2010. Note that the data in Vietnam and Cambodia are interpolated due to the lack of CLIMAT report or climatological normal.

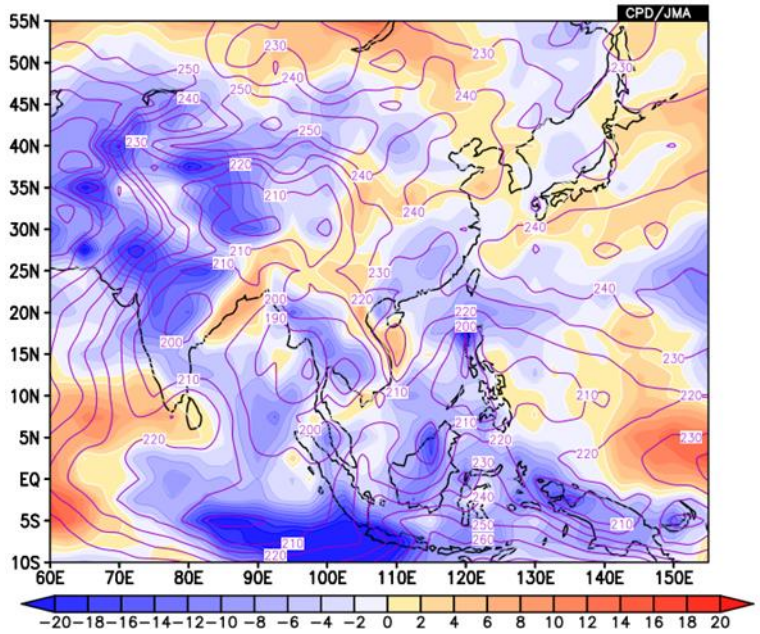

Figure 11 Four-month mean OLR and its anomaly for June–September 2016
The contours indicate OLR at intervals of 10 W/m^2, and the color shading denotes OLR anomalies from the normal (i.e., the 1981–2010 average). Negative (cold color) and positive (warm color) OLR anomalies show enhanced and suppressed convection compared to the normal, respectively. Original data are provided by NOAA.

TC activity and tracks in August were especially notable. A total of seven TCs formed, with six approaching or making landfall on East Asia and five approaching or making landfall on mainland Japan (climatological normal: 1.7). Some of these TCs formed to the southeast of Japan and moved northward toward the country. This was unusual for the time of year, when most TCs in the region move westward along the southern edge of the North Pacific Subtropical High. These unusual track characteristics resulted in three TC landfalls on Hokkaido for the first time since 1951.

Table 1 Tropical cyclones forming over the western North Pacific from June to September 2016

Number ID	Name	Date (UTC)	Category[1)]	Maxumum wind[2)] (knots)
T1601	Nepartak	7/3–7/9	TY	110
T1602	Lupit	7/23–7/24	TS	40
T1603	Mirinae	7/26–7/28	STS	55
T1604	Nida	7/30–8/2	STS	60
T1605	Omais	8/4–8/9	STS	60
T1606	Conson	8/9–8/14	TS	45
T1607	Chanthu	8/13–8/17	STS	55
T1608	Dianmu	8/17–8/19	TS	40
T1609	Mindulle	8/19–8/23	TY	65
T1610	Lionrock	8/21–8/30	TY	90
T1611	Kompasu	8/20–8/21	TS	35
T1612	Namtheun	9/1–9/4	TY	70
T1613	Malou	9/6	TS	40
T1614	Meranti	9/10–9/15	TY	120
T1615	Rai	9/12–9/13	TS	35
T1616	Malakas	9/12–9/20	TY	95
T1617	Megi	9/23–9/28	TY	85
T1618	Chaba	9/29–10/5	TY	115

Note: Based on information from the RSMC Tokyo-Typhoon Center.
1) Intensity classification for tropical cyclones
TS: tropical storm, STS: severe tropical storm, TY: typhoon
2) Estimated maximum 10-minute mean wind

3. Monsoon activity and atmospheric circulation

Convective activity (inferred from OLR) averaged for June – September 2016 was enhanced from the eastern Indian Ocean to the Maritime Continent, over the area from the Bay of Bengal to the southwestern Indochina Peninsula and from southern China to the seas northeast of the Philippines, and was suppressed over the western part of the equatorial Pacific (Fig. 11). OLR index data (Table 2) indicate that the overall activity of the Asian summer monsoon (represented by the SAMOI (A) index) was near normal until August and above normal in September. The most-active convection area was shifted westward of its normal position until July (see the SAMOI (W) index.).

In the upper troposphere, the Tibetan High was stronger than normal over its northeastern part (Figure 12 (a)). In the lower troposphere, monsoon circulation over the Indian Ocean was stronger than normal and cyclonic circulation anomalies straddling the equator were seen over the area from the Indian Ocean to the Maritime Continent (Figure 12 (b)). Zonal wind shear between the upper and lower troposphere over the North Indian Ocean and southern Asia (Figure 13) remained above normal, indicating stronger-than-normal monsoon circulation from mid-May onward (except in the second half of July and the first half of late August).

Convective activity over the Maritime Continent was enhanced throughout the summer monsoon season, while to the east of the Philippines it was suppressed in the first half of the season and enhanced in the second half (Fig. 14). In the lower troposphere, cyclonic circulation associated with a deep monsoon trough was clearly seen over the seas to the southeast of Japan in August in association with enhanced convective activity over the western North Pacific.

(Section 1 and 2: Kenji Kamiguchi, 3: Hitomi Saitou, Climate Prediction Division)

Table 2 Summer Asian Monsoon OLR Index (SAMOI) values observed from May to October 2016

Asian summer monsoon OLR indices (SAMOI) are derived from OLR anomalies from May to October. SAMOI (A), (N) and (W) indicate the overall activity of the Asian summer monsoon, its northward shift and its westward shift, respectively. SAMOI definitions are as follows: SAMOI (A) = (-1) × (W + E); SAMOI (N) = S – N; SAMOI (W) = E – W. W, E, N and S indicate area-averaged OLR anomalies for the respective regions shown in the figure on the right normalized by their standard deviations.

	Summer Asian Monsoon OLR Index (SAMOI)		
	SAMOI (A): Activity	SAMOI (N): Northward-shift	SAMOI (W): Westward-shift
May 2016	0.4	-0.8	1.2
Jun. 2016	0.3	-0.5	1.0
Jul. 2016	-0.4	0.1	1.2
Aug. 2016	0.5	0.3	-0.9
Sep. 2016	1.6	0.8	0.0
Oct. 2016	1.1	-0.9	-0.5

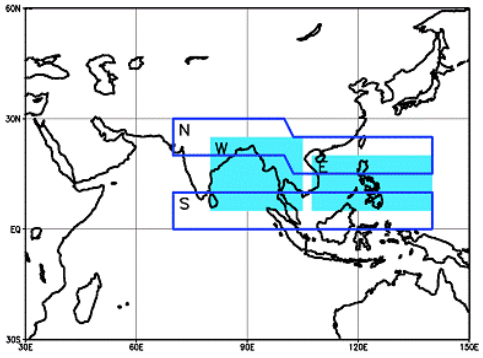

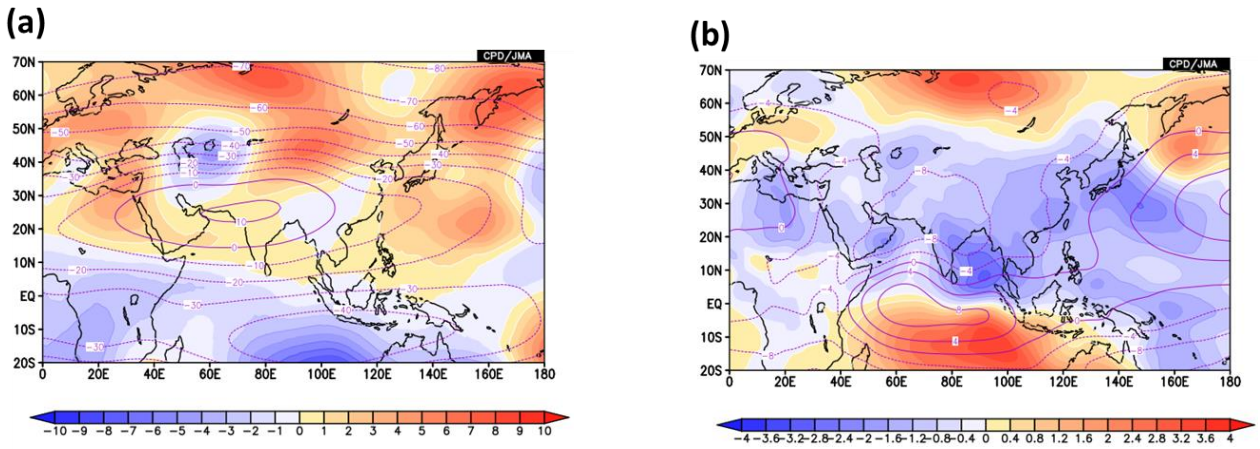

Figure 12 Four-month mean stream function and its anomaly for June – September 2016

(a) The contours indicate the 200-hPa stream function at intervals of 10×10^6 m^2/s, and the color shading indicates 200-hPa stream function anomalies from the normal. (b) The contours indicate the 850-hPa stream function at intervals of 4×10^6 m^2/s, and the color shading indicates 850-hPa stream function anomalies from the normal. The base period for the normal is 1981 – 2010. Warm (cold) shading denotes anticyclonic (cyclonic) circulation anomalies in the Northern Hemisphere, and vice-versa in the Southern Hemisphere.

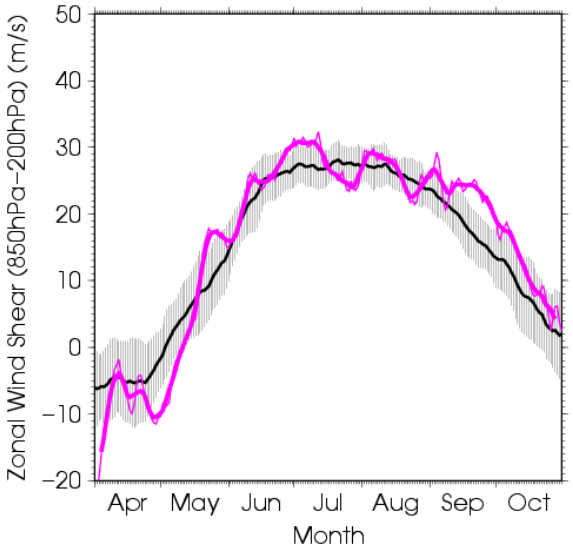

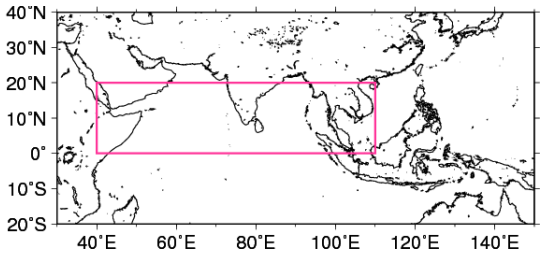

Figure 13 Time-series representation of the zonal wind shear index between 200-hPa and 850-hPa averaged over the North Indian Ocean and southern Asia (the region enclosed by the pink rectangle in the right figure: equator – 20°N, 40°E – 110°E)

The zonal wind shear index is calculated after Webster and Yang (1992). The thick and thin pink lines indicate seven-day running mean and daily mean values, respectively. The black line denotes the normal (i.e., the 1981 - 2010 average), and the gray shading shows the range of the standard deviation calculated for the time period of the normal.

(a) June

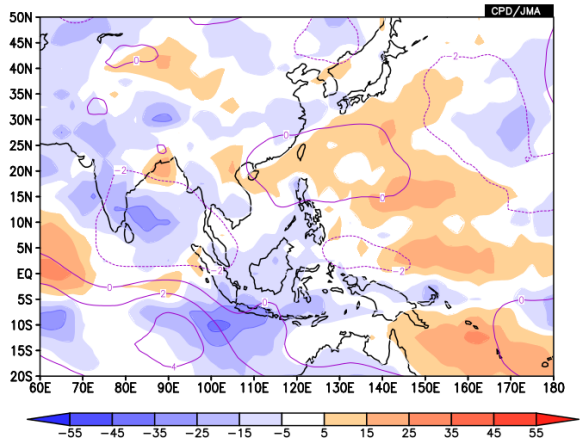

(b) July

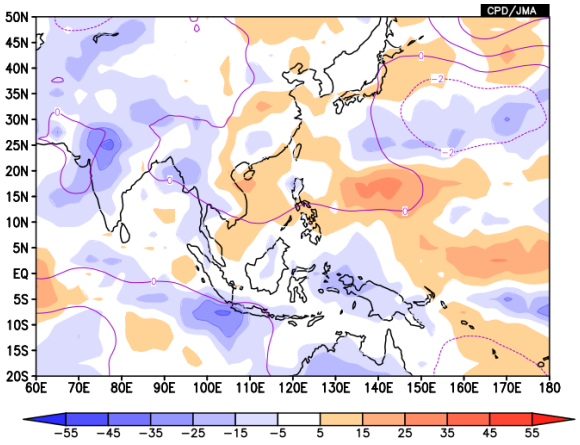

(c) August

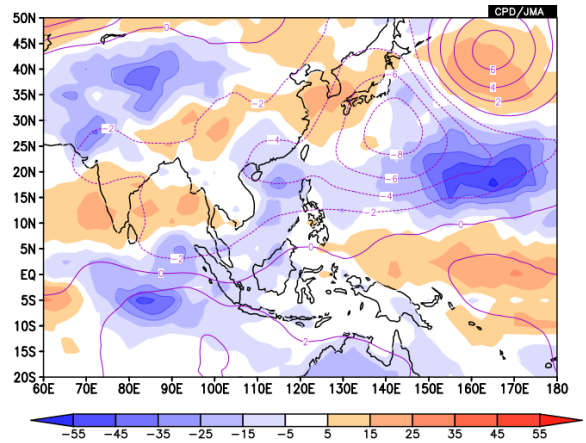

(d) September

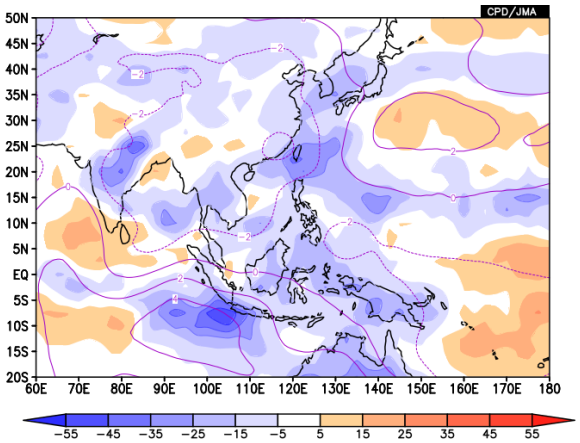

Figure14 Monthly mean anomalies of OLR (shading at intervals of 10 W/m^2) and 850-hPa stream function (contour at intervals of 2×10^6 m^2/s) for (a) June, (b) July, (c) August and (d) September 2016

References

Webster, P. J. and S. Yang, 1992: Monsoon and ENSO: Selectively interactive systems. *Quart. J. Roy. Meteor. Soc.*, **118**, 877 – 926.

Status of the Antarctic Ozone Hole in 2016

The Antarctic ozone hole in 2016 remained at the average size observed over the last ten years.

Over the last 30 years, the Antarctic ozone hole has appeared every year in Austral spring with a peak in September or early October. It is generally defined as the area in which the total ozone column is equal to or less than 220 m atm-cm.

JMA analysis based on Aura OMI data indicates that the Antarctic ozone hole in 2016 appeared in mid-August and expanded rapidly from late August to mid-September, reaching its maximum size for the year on 28 September. At this time, it covered 22.7 million square kilometers (see the upper-left panel in Figure 15), which is 1.6 times as large as the Antarctic Continent. Its maximum size was equivalent to the average observed over the last ten years and less than that of 2015, which was the fourth-largest since 1979 (upper-right panel).

The ozone layer acts as a shield against ultraviolet radiation, which can cause skin cancer. The ozone hole first appeared in the early 1980s and reached its maximum size of 29.6 million square kilometers in 2000. The Antarctic ozone hole has caused significant changes in Southern Hemisphere surface climate in the summer, and will continue to appear at least until the middle of the century according to WMO/UNEP Scientific Assessment of Ozone Depletion: 2014 Assessment for Decision-Makers. Close observation of the ozone layer on a global scale (including that over the Antarctic region) remains important.

(Atsuya Kinoshita,
Ozone Layer Monitoring Center)

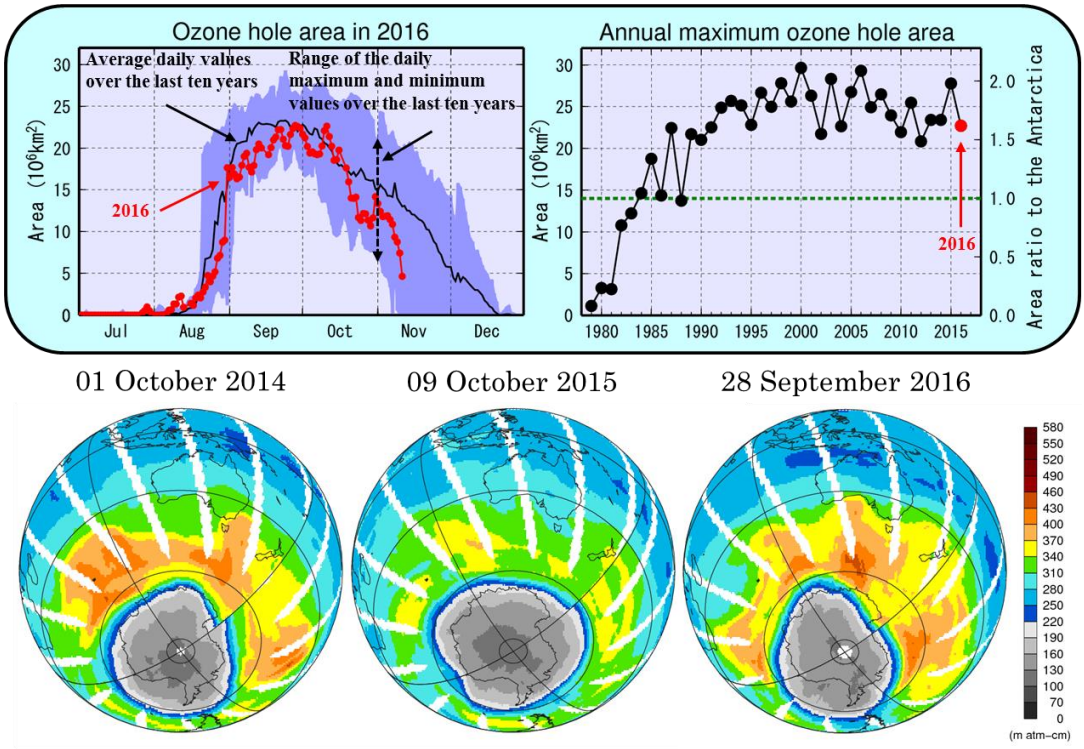

Figure 15 Antarctic ozone hole characteristics in 2016

(Upper left) Time-series representation of the daily ozone-hole area for 2016 (red line) and the 2006–2015 average (black line). The blue shading area represents the range of daily minima and daily maxima over the past 10 years.

(Upper right) Interannual variability in the annual maximum ozone-hole area

(Bottom) Snapshots of total column ozone distribution on the day recorded the annual maximum ozone hole area for the last three years; the ozone hole is shown in gray. These panels are based on data from NASA satellite sensors of the ozone monitoring instrument (OMI).

TCC contributions to SASCOF-9

The Department of Meteorology and Hydrology (DMH, Myanmar) hosted the ninth session of the South Asian Climate Outlook Forum (SASCOF-9) on 27 and 28 September 2016 in Nay Pyi Taw. The session provided a platform for its 40 or so attendees to discuss seasonal climate conditions in the upcoming Northeast Monsoon period (Oct. 2016 to Feb. 2017). First, representatives of WMO's Global Producing Centers for Long-range Forecasts (GPCs), including Mr. Shoji Hirahara from GPC Tokyo, provided dynamical model outlooks with focus on the evolution of cool ocean conditions in the eastern tropical Pacific during winter 2016/2017. This was followed by detailed country-scale outlooks from National Meteorological and Hydrological Services (NMHSs) of South Asia. One of the key outcomes of the forum was a consensus forecast for the eastern tropical Pacific suggesting equal likelihoods of 1) ongoing cool neutral ocean conditions to continue and 2) a borderline La Niña event to develop in winter.

The forum was held in conjunction with the second session of the Climate Services Users Forum for Agriculture (CSUF-Ag2; 28 – 29 September), at which experts from agricultural administrations and research centers shared their experiences of using climate information in the agricultural sector. Mr. Hirahara was also involved in active discussions here to support better use of information for climate-smart agricultural practices.

(Shoji Hirahara, Tokyo Climate Center)

TCC Training Seminar on Primary Modes of Global Climate Variability and Regional Climate

JMA's Tokyo Climate Center (TCC) assists National Meteorological and Hydrological Services (NMHSs) in improving their climate services. The Center's two major activities in this regard involve providing basic climate data and products to NMHSs through its website and assisting with capacity development at NMHSs in the Asia-Pacific region. TCC holds annual training seminars as part of capacity development activities related to its role as an RCC in the WMO RA II area. In addition to running annual training seminars, it arranges expert visits to and hosts visitors from NMHSs to promote the effective transfer of technology and discuss the support for climate services.

In 2016, TCC held the Training Seminar on Primary Modes of Global Climate Variability and Regional Climate from 14 to 18 November 2016 at JMA Headquarters in Tokyo. The event was attended by 14 experts from NMHSs in Bangladesh, Cambodia, Hong Kong (China), Indonesia, Lao People's Democratic Republic, Malaysia, Mongolia, Myanmar, Pakistan, the Philippines, Singapore, Sri Lanka, Thailand and Viet Nam. The seminar focused on enhancing expertise for the identification of statistical relations between primary modes of global-scale climate variability and regional/local climates and on improving the capacity for related interpretation from a meteorological perspective. The course included lectures and practical exercises using data, products and a

web-based application tool available on the TCC website as well as in-situ observation data brought by participants.

At the end of the seminar, all attendees gave presentations on the relationship between global-scale climate variability and regional/local climate conditions in their own countries and related meteorological interpretation and engaged in fruitful discussions with lecturers and others present. The content of the lectures is available on the TCC website at

http://ds.data.jma.go.jp/tcc/tcc/library/library2016.html.

(Atsushi Goto, Tokyo Climate Center)

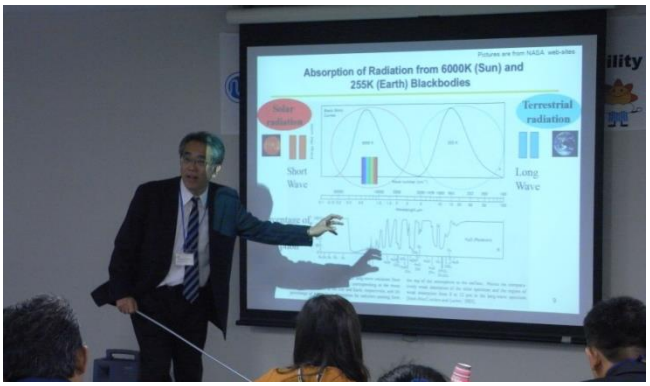

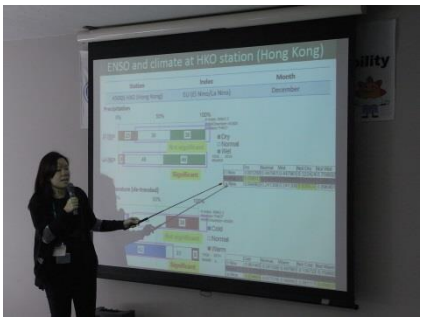

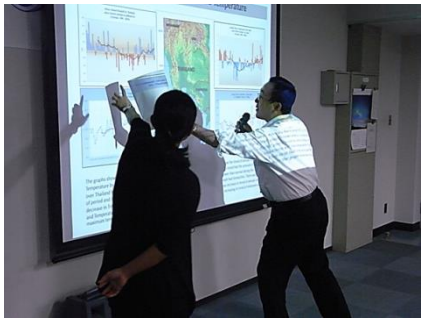

Any comments or inquiry on this newsletter and/or the TCC website would be much appreciated. Please e-mail to tcc@met.kishou.go.jp.

(Editors: Kiyotoshi Takahashi, Atsushi Goto and Yasushi Mochizuki)

Tokyo Climate Center (TCC), Japan Meteorological Agency
Address: 1-3-4 Otemachi, Chiyoda-ku, Tokyo 100-8122, Japan
TCC Website: http://ds.data.jma.go.jp/tcc/tcc/index.html